

Acetone Condensation Reaction on Acid Catalysts

A. G. Panov and J. J. Fripiat¹

Department of Chemistry and Laboratory for Surface Studies, University of Wisconsin-Milwaukee, Milwaukee, Wisconsin 53201

Received December 22, 1997; revised March 23, 1998; accepted April 28, 1998

The condensation reaction of acetone on alumina and acid zeolites has been followed by FTIR. Under identical conditions, the reaction rate is faster on alumina, and the condensation goes beyond the formation of mesityl oxide. Zeolites without nonframework aluminum are poor catalysts. On HZSM-5 the reaction is about two orders of magnitude slower than on USY at 105°C. From these data, it appears that Lewis sites, even if they bound acetone less energetically than Brønsted sites, are responsible for the activation of the molecule. On alumina, the reaction would take place between gas phase acetone and acetone adsorbed on Lewis sites. On zeolites with nonframework aluminum and, thus, with Lewis sites, the reaction would involve acetone molecules adsorbed on Brønsted and Lewis sites, the activation occurring on the Lewis site. © 1998 Academic Press

INTRODUCTION

Numerous studies have been devoted to the adsorption-transformation of acetone on oxides (1–3) and acid catalysts (4–10). IR (1–7) and NMR (8–13) techniques were used to describe adsorption complexes of acetone on surface sites. The formation of an 1 : 1 adsorption complex between acetone and Brønsted acid sites of HZSM-5 was reported by several research groups (9, 12). Biaglow *et al.* (11) pointed out that localized adsorption complexes exist on the surface of acidic ZSM-5 zeolites at low coverages (less than one acetone per one aluminum atom in framework position). At higher coverages, acetone becomes more mobile which is proven by the disappearance of spinning sidebands, present at lower coverages, in the ¹³C NMR spectrum.

Both IR and NMR technique were also used to study the reactivity of acetone complexes with zeolite acid sites toward aldol condensation (6–10). The chemistry of aldol condensation of acetone over a variety of zeolites at coverages higher than one acetone per Brønsted site and different temperatures was detailed by Haw and co-workers (9). For HZSM-5, formation of mesityl oxide was observed even at room temperature. Biaglow *et al.* (10) studied the transformation of acetone over HZSM-5 zeolites at different coverages and temperature. The mobility of adsorbed acetone

seems to play a primary role in the bimolecular condensation (10). When a localized complex between acetone and Brønsted acid sites is formed, the transformation in mesityl oxide does not occur. By increasing the coverage or the temperature of the system (100°C), acetone dehydrates to form mesityl oxide. The diacetone alcohol, the aldol dimerization product of acetone is not observed (6–10).

The present study has been preceded by a paper dealing mainly with the assignment of the spectral features of adsorbed acetone and mesityl oxide. Mesityl oxide is easily identified as the first observable condensation product. It is, by the way, amusing that this identification is relatively recent. For instance, Lercher (1), who has extensively studied the adsorption of acetone on several oxides and mixed oxides using IR has wrongly assigned to carboxylate, bands which, in fact, were due to mesityl oxide. Table 1 shows the band assignments essential for the present work. It summarizes the conclusions of the preliminary paper (14).

Besides the C=O and C=C stretching vibrations which are the most important for this work, CH bendings are also observed between 1470 and 1300 cm⁻¹. A band at ~1450 cm⁻¹ is characteristic of mesityl oxide. A shoulder at 1471 cm⁻¹ seems to be the result of the ring vibration of mesitylene (14).

The assignment of a band at ~1700 cm⁻¹ to acetone (Ac) interacting weakly with silanol comes from the observation that the intensity of the zeolite OH stretching at 3740 cm⁻¹ decreases as absorption of acetone at ~1700 cm⁻¹ increases (14). This band is observed easily in USY and HZSM-5 zeolites. In H-mordenites in which the extent of dealumination is negligible, the main CO stretching vibrations of adsorbed Ac are at 1679 and 1645 cm⁻¹ with widths of 28 and 49 cm⁻¹, respectively. These bands are attributable to two different kinds of bridging Si-OH-Al sites with different acid strengths, the most shifted one being the strongest (14). These are also observable in HZSM-5 and USY.

The width and frequency distribution of the CO stretching bands of adsorbed acetone support the early conclusion by Hair (15) that acetone is not a good probe for acid sites. It would be physically more meaningful to consider a continuum in the distribution of the strengths of electron acceptor sites with which the carbonyl interacts, the spread

¹ To whom correspondence should be addressed.

TABLE 1

Assignments of the C=O Stretch of Acetone (Ac) and Mesityl Oxide (MO) Adsorbed on Brønsted (B) and Lewis Acid Sites (L) on Acid Catalysts at 105°C. Zeolites Bridging OHs Acting as Brønsted Sites Are Designated as B₁ whereas the Weakly Acidic Bridging OHs Are Designated as B₂. WHH: Full Width at Half-Height

Acetone				
Sample and sites	C=O stretch (cm ⁻¹)	WHH (cm ⁻¹)		
Physisorbed	1714–1720	12–15		
SiOH	1700–1705	22		
L	1690–1702	27		
B ₂	1679–1682	27		
B ₁	1652–1655	44		
Mesityl oxide				
Sample and sites	C=O stretch (cm ⁻¹)	WHH (cm ⁻¹)	C=C stretch (cm ⁻¹)	WHH (cm ⁻¹)
B HM ^a and HZSM-5 ^b	1617	43	1557	71
B ₁ ; HY ^c and B ₁ ; USY ^d	1631	24	1565	57
B ₂ ; HY ^e	1659	18	1594	32
B; USY	1632	30	1565	55
L; Alumina ^e	1673	21	1589–1603	42
L; (USY)	1676	21	1604	42

^a H-mordenite.

^b HZSM-5.

^c H near faugasite Y.

^d Ultrastable Y.

^e Nanosized alumina. SiOH represents the nonbridging OH group; its OH stretch is usually between 3700 and 3750 cm⁻¹.

of stretching frequency being from about 1700 to 1650 cm⁻¹. Lewis, as well as Brønsted sites, are included in this broad distribution.

As stated earlier, mesityl oxide is a better probe than acetone for acid sites because of the larger frequency shifts of the conjugated C=C, C=O with respect to the electron acceptor site strength. The relative shifts of the CO and CC vibrations are affected to the same extent by this interaction, but the bands are better resolved because they are more spread out than in acetone.

The shifts of the C=O and/or C=C bands scale as the strength of the Brønsted sites. The shifts in HZSM-5 and HM are the largest, whereas in HY they are the smallest. This is in agreement with activity for the steady-state transformation of pentane. On HZSM-5, HM, USY, and HY pretreated at 500°C, the activity scales as 100, 18.5, 13, and 0.85, respectively (16). Earlier studies on the low-temperature adsorption of carbon monoxide on acid or acid and dealuminated zeolites had shown two CO stretching bands with

frequencies at 2175 ± 2 cm⁻¹ or at 2163 cm⁻¹ in HZSM-5 and USY (17). These observations suggest that carbon monoxide interacts with two kinds of OH. Indeed, the bridging Si–OH–Al are distributed among three populations, depending upon the number *n* of next-nearest-neighbor Al atoms (0 < *n* < 3). Isolated Al sites (*n* = 0) are bearing the most acidic OH (18, 19). The first and second population (*n* = 1) are in cluster Si–1Al while the third one is in cluster (Si–*n*Al with *n* > 1), either Si–2Al...Si–4Al. Only the first and second populations are actual Brønsted sites, in the sense that upon exposure to NH₃ they transform into NH₄. The OHs in cluster (Si–*n*Al), *n* > 1 are not Brønsted sites (no proton transfer to NH₃) but they can hydrogen-bond NH₃.

The B₁ band at ~1650 cm⁻¹ has been assigned to the acetone carbonyl in a H-bonded complex with the most acidic OH sites. The linear regression between the number of acetone in the B₁ band and the number of Brønsted sites supports this agreement (14). The C=O and C=C band assignments of adsorbed MO shown in Table 1 are in good agreement with those in Ref. 6 (see two bottom rows) which were obtained for Brønsted sites in HZSM-5. The bands assigned to Lewis sites in Ref. 6 were obtained on a calcined HZSM-5, and their frequencies are 24 cm⁻¹ lower than those we have obtained on amorphous alumina or on nonframework aluminas in USY.

Now, turning our attention toward the catalytic activation of acetone, because the transformation of acetone by liquid acids is well documented (20), the role of Brønsted acid sites has been particularly emphasized (9, 10, 13). However, the role of Lewis sites deserves some attention because it is difficult to prepare an acid zeolite without having some dealumination. Lewis sites are present on nonframework alumina within the zeolite microcrystals (21). For example, in hydrocarbon cracking and isomerization, the presence of nonframework alumina (e.g., the presence of Lewis acid sites) affects the catalytic activity (22).

The aim of this paper is to reexamine the condensation reaction. The reason for reexamining the problem stems from the observation that on the surface of alumina, rich in Lewis sites, condensation of acetone occurs very rapidly at room temperature. It even proceeds to a very limited extent at –60°C. At room temperature, the reaction goes beyond the formation of mesityl oxide because spectral features, which could be caused by isophorone and aromatics have been observed. Therefore, Lewis sites appear to be at least as active as Brønsted sites, yet, it seems that this aspect has been neglected in recent times.

Before continuing, we want to outline two apparently important omissions in the present contribution, which concern either the formation of enol or of higher condensation products. We have not been able to characterize enol, in spite of a careful search. Moreover, we disagree with several of the assignments of bands, which have been attribute

to enol and, which, according to us, belong to either mesityl oxide or acetone. For instance, Hanson *et al.* (2) suggested that a band at 1596 cm^{-1} is caused by acetone enolate. We believe that this band is caused by the C=C stretching of MO on Lewis sites because it develops progressively with a band at 1673 cm^{-1} (C=O on Lewis sites) upon adsorbing MO on alumina.

Because the reaction temperature in this work never exceeds 105°C , the formation of higher condensation products must have been limited. On alumina according to V. Bell (8), the formation of isophorone occurs after 1.5 h at 72°C , and it is only above 200°C that mesitylene appears. Hanson *et al.* (2) have observed a strong IR band at 1638 cm^{-1} on adsorbing isophorone on γ -alumina at room temperature. In several of our spectra, for instance, in adsorbing MO on alumina, a shoulder is observed at that frequency, and it is not that of an impurity. It could be caused by relatively small amounts of physically adsorbed MO because it is at $\sim 1635\text{ cm}^{-1}$ that the CO stretching of MO shows up.

Among the objectives of this study, the determination of the nature of the active sites is a first priority. The primary condensation reaction is a bimolecular reaction, and as mentioned by others (6, 10), it has been suggested that it occurred between acetone adsorbed on Brønsted sites (activated carbonyl group) and mobile (eventually physisorbed) acetone. In the presence of Lewis sites, it could well happen between acetone adsorbed on Brønsted sites and acetone adsorbed on Lewis sites, the latter adsorption being much less energetic than the first.

EXPERIMENTAL

Catalysts. All catalysts used for the adsorption studies have been described earlier. The nanosized amorphous, rich in coordination defects, alumina has been prepared by a sol-gel process (23) and calcined at 600°C . Its Lewis acidity has been carefully characterized (24–26). The total number of Lewis sites is 0.4 meq/g , and the surface area is between 300 and $350\text{ m}^2/\text{g}$. USY is a commercial (PQ) catalyst. USY5F and USY10F are the results of further USY dealumination using NH_4F (29). In USY5F both the numbers of Brønsted and Lewis sites are reduced to less than 50% of the initial content in USY, whereas in USY10F the reduction reaches about 80%. The HZSM-5 sample is from PQ, and it was prepared as indicated in Ref. 24. The preparation and characterization of HM and DHM700 have been described in Ref. 26.

Table 2 shows the Si/Al ratios obtained from ^{29}Si NMR and the numbers of Lewis and Brønsted acid sites. In order to minimize the dealumination process and, therefore, the number of Lewis sites, HY, HM and HZSM5 were deammoniated at 400°C in the IR cell before use. The dealuminated samples were dried in the IR cell by outgassing at 500°C for 5 h under a 10^{-5} Torr residual pressure and pretreated

TABLE 2
Number of Acid Sites on the Catalyst Used Here: L: Lewis and Brt: Total Brønsted Obtained from NH_3 Chemisorption (mmol/g) (21, 24)

Catalyst	L	Brt	NMR Si/Al
Alumina	0.4	—	—
USY	1.43	1.42	4.9
HY(580)	1.32	0.98	5
USY5F	0.78	0.62	14
DHM700 and VG700	0.82	0.83	14
USY10F	0.33	0.23	59
HM	0.38	1.25	9.8
HY	n/a	>1.6	(2.55) ^a
HZSM5	~ 0	0.83	17.5

^a Dealumination assumed to be negligible.

by 20 Torr oxygen at the same temperature. The ^{29}Si NMR spectra were recorded on samples reequilibrated with atmospheric moisture.

Reagents. Acetone (94.9%) and mesityl oxide (99%) were Aldrich products which were dried over 4A molecular sieve (Ac) or MgSO_4 (MO) and purified by repeated freezing and thawing.

Instrument. The FTIR spectra were obtained with a Perkin Elmer 1800 operating in the absorbance mode. The spectral resolution was 2 cm^{-1} . The stainless steel cell is fitted with KBr windows and can be outgassed up to 600°C or it can be cooled at -190°C . The weight of the pellets is about 14 mg/cm^2 . All spectra were recorded at the reaction temperature.

A quadrupole mass spectrograph, linked to the infrared cell by a leak valve, permits us to monitor the formation of water or the disappearance of acetone from the gas phase.

The Reaction. The reaction temperature has been, in all cases, 105°C . Two different starting amounts of reagent were used. The so-called large dose corresponded to a number of acetone molecules ($\sim 3\text{ mmol/g}$) larger than the number of Brønsted sites (Table 2). The small dose ($\sim 0.4\text{ mmol/g}$) is always smaller than the number of Brønsted sites. The large dose is larger than the sum of Brønsted and Lewis sites.

The FTIR spectra were collected every 20 s in the case of alumina (4 scans) (fast reaction) and every 5 min in the case of zeolites (20 scans) (slower reaction).

The formation of mesityl oxide was monitored in deconvoluting the spectra in order to record the integrated intensity of the C=C stretch, which is observed between 1557 and 1565 cm^{-1} on the B_1 Brønsted sites or at $\sim 1600\text{ cm}^{-1}$ on Lewis sites. Examples of deconvolution and values of the extinction coefficients were given in the preliminary paper (14).

It should be emphasized that the C=C stretch in further condensation products such as phorone could overlap with the C=C bands assigned to mesityl oxide. Adsorbed isophorone has been identified by a band at 1638 cm^{-1} (2). The low vapor pressure of phorone makes it difficult to study its spectrum in the adsorbed state. Condensation in aromatics is also possible as suggested by Xu *et al.* (9).

Because the discussion will focus mainly on the initial rate of reaction and because the temperature did not exceed 105°C , it can be assumed that, for zeolites, the amount of higher condensation products is negligible, with respect to that of the main reaction product (e.g., mesityl oxide).

The consumption of acetone was followed by the decrease of the acetone C=O stretching bands. The integrated intensities, converted into concentration using the extinction coefficients of CO on L, B₁ and B₂ and eventually SiOH sites were obtained through the deconvolution of the complex band into three components (14). In fact, because the CO stretch of acetone on Lewis sites and on SiOH overlap, only three components were used. The sum of the concentrations in acetone adsorbed on these sites is called Acs (s of adsorbed acetone, whatever the site).

RESULTS

Figures 1–4 show examples of the evolution of the FTIR spectra over time during the reaction of large and small doses of acetone at 105°C on different catalysts. These eight sets of spectra are representative for all the experiments which will be described and the results which will be discussed in the present contribution. From the deconvolution of these spectra and using the specific absorbances reported earlier (14), follow the quantitative data reported in Figs. 5 and 6 and discussed in the last section.

On alumina the reaction is fast even in the presence of small doses (Fig. 1A), whereas on zeolite without nonframework aluminum (Fig. 2B), there is practically no reaction. If the zeolite contains nonframework aluminum (NFAI), the reaction rate is measurable even with small doses (Figs. 1B and 2A). With large doses, the reaction proceeds quite rapidly on zeolites (Figs. 3 and 4). Still the absence of NFAI slows down the reaction (Fig. 3B). On alumina, the reaction rate is too fast to be measured with large doses at 105°C .

Note that, sometimes, the equilibrium between the gas phase and the solid is not reached at the time the initial spectrum is taken. This is the case in Figs. 1B, 2A, and 4B.

The frequencies of the Ac CO and of the MO CO and CC stretching vibrations are indicated in the figures. They differ slightly from those shown and assigned in Table 1 corresponding to room temperature spectra. The shift of the Mo C=C band, for instance, is about 8 cm^{-1} toward lower frequencies between room temperature and 105°C on USY.

On alumina (Fig. 1) besides the line assigned at the C=C stretch of MO on Lewis sites (at $\sim 1591\text{ cm}^{-1}$), two bands are growing at 1620 and 1471 cm^{-1} , respectively. A weak band at $\sim 1471\text{ cm}^{-1}$ is observed in zeolites with large contents in NFAI (Figs. 3A and 4A), but the corresponding condensation product is formed in much smaller amounts.

Water is a product of the reaction which can poison the catalyst by reacting with Lewis acid sites. Not only does H₂O chemisorb on L sites where it competes with acetone, but also upon dissociative chemisorption it decreases the number of coordinately unsaturated aluminum in alumina and in the nonframework aluminum species in zeolites (28). The mass 18 signal is easily detected by the quadrupole; it increases with time at the same rate as the acetone 43 and 58 signals disappear, but it is always smaller than

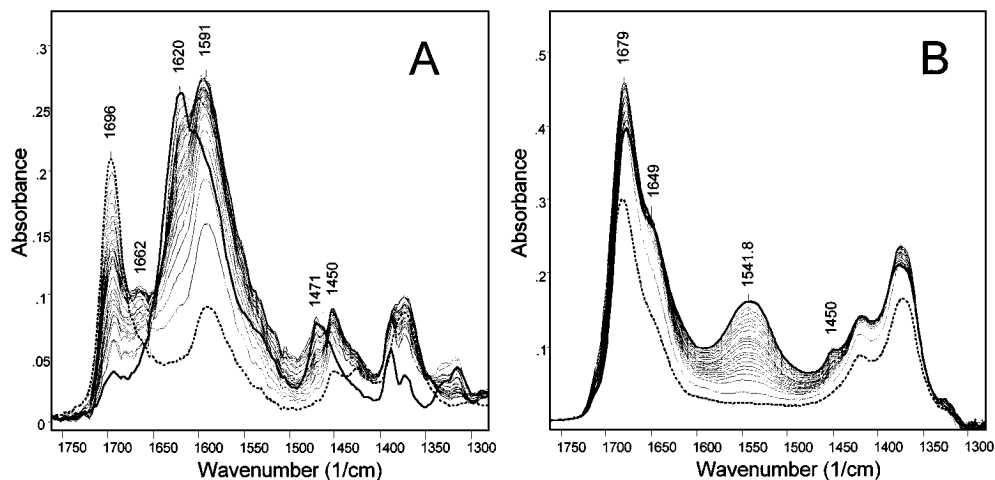


FIG. 1. Evolution of infrared spectra of small doses (see text) of Ac adsorbed on alumina (A) and on DHM700 (B) at 105°C with time. In (A) the spectra are recorded every 20 s (4 scans per spectrum) and in (B) they are repeated every 5 min (24 scans per spectrum). The initial spectrum is always indicated by a dotted line; the final one, by a solid line.

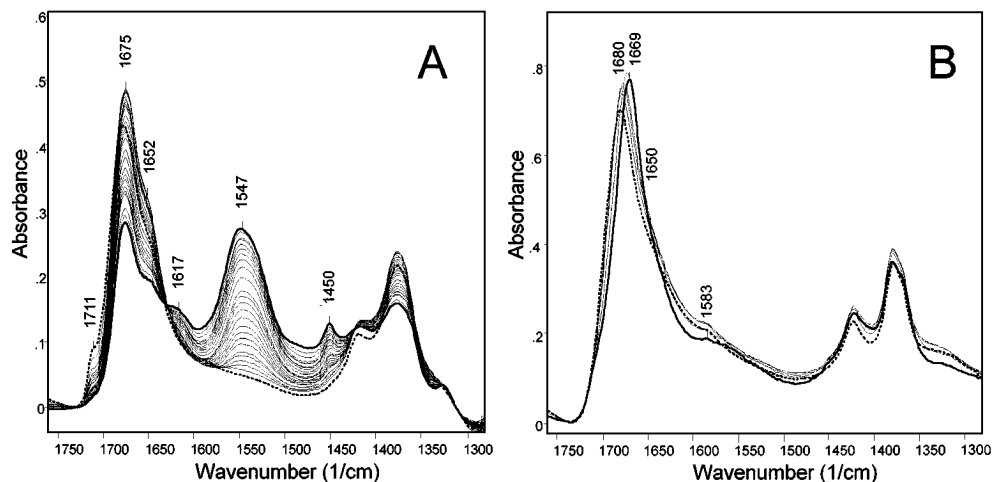


FIG. 2. Evolution of infrared spectra of small doses of Ac adsorbed on USY (A) and on HY (B) at 105°C with time. The spectra are recorded every 5 min (24 scans per spectrum).

expected. In other words, a fraction of the water is adsorbed or chemisorbed. The obvious domain of frequency to look for water is in the bending deformation region (e.g., near 1620 cm^{-1}). A band is observed in this region, especially on catalysts in which the yield in MO is high (Figs. 1A, 2B, 3A and 4A). Unfortunately, the region of the H_2O bending mode is also that of the $\text{C}=\text{O}$ stretching of MO on Brønsted sites (Table 2). As a consequence, the formation of water cannot be monitored. We have observed on USY, for instance, that the intensity of the 1621 cm^{-1} band, if assigned to MO, overestimates the yield in MO. This goes in the right direction, if the MO $\text{C}=\text{O}$ stretching and H_2O bending overlap.

Without too optimistic anticipation, we have tried to observe eventual new OH stretching signals above 3000 cm^{-1} as reaction proceeds on alumina or zeolite with NFAl. In

fact, it is impossible to distinguish between the initial OH shifted upon interaction of the various proton acceptors in the system and “new” OH in the stretching region.

The progress of the reaction will be appreciated by the development of the band assigned either to $\text{C}=\text{C}$ on Brønsted sites in zeolites or to $\text{C}=\text{C}$ on Lewis sites on alumina. On bridging OH sites, as shown in Table 1, depending upon the strength of the site, the band is between ~ 1550 and 1580 cm^{-1} .

In order to obtain information on the Ac consumption, the band encompassing the $\text{C}=\text{O}$ stretch of Ac interacting with the B_1 and B_2 sites was integrated. The integrated intensity between ~ 1698 and 1715 cm^{-1} was considered as representing Ac interacting either with Lewis sites or terminal silanols, namely, Ac in weaker interaction with the surface but still adsorbed at 105°C. On alumina, Ac

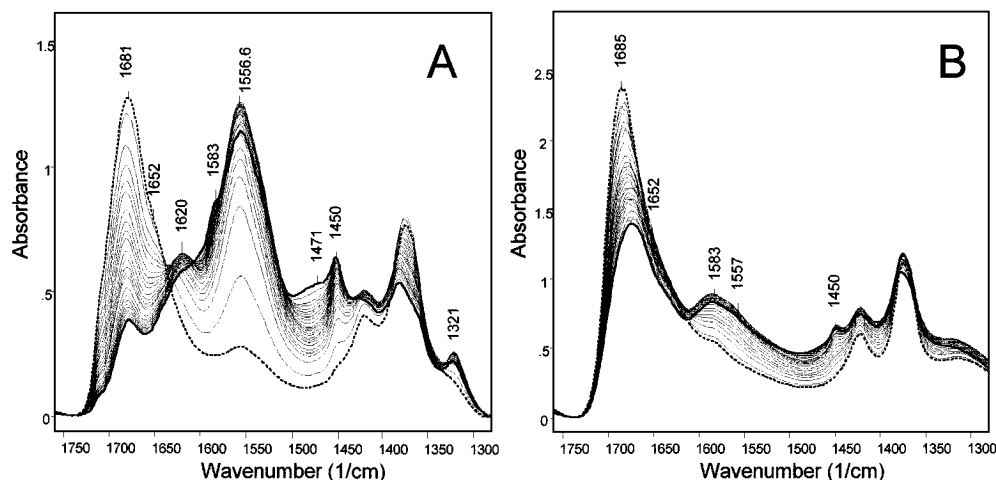


FIG. 3. Evolution of infrared spectra of large doses of Ac adsorbed on USY (A) and HY (B) at 105°C with time. (See Fig. 1 caption.)

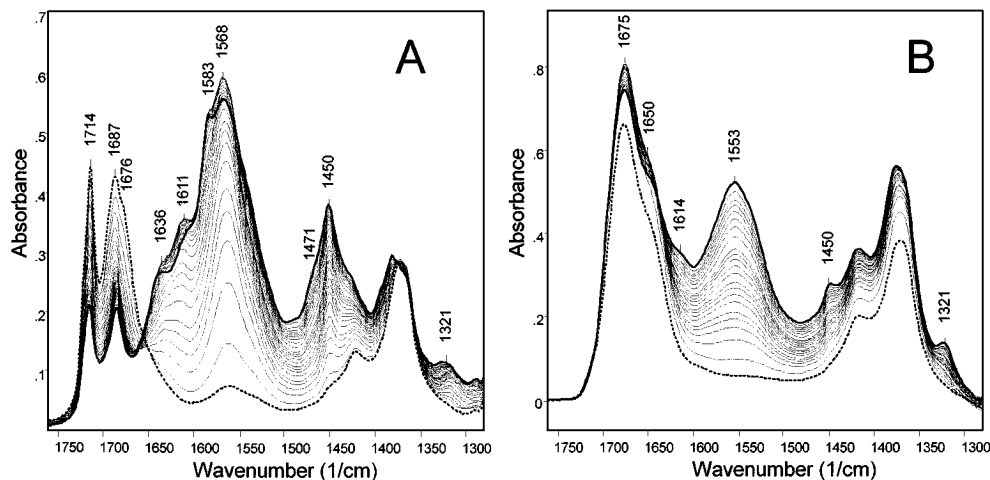


FIG. 4. Evolution of infrared spectra of large doses of Ac adsorbed on USY10F (A) and on DHM700 (B) at 105°C with time. (See Fig. 1 caption.)

is adsorbed on Lewis sites only, and the CO stretch is at 1695 cm^{-1} (Fig. 1A).

The evolutions of the surface concentrations over time are shown in Figs. 5 and 6. For zeolites, the sum of the amounts of reagent and of the reaction product (multiplied by 2) on the surface reaches a constant level after about 100 min (Figs. 5A and 6B).

On alumina, the same trend is observed if the C=C vibration of MO is considered, but the sum of twice the surface MO concentration plus the surface reagent concentration starts decreasing after about 5 min reaction. A decrease of the MO C=O stretching band intensity occurs beyond 5 min; it is not observed for zeolites. Most probably, the

condensation in higher polymer is responsible for the decrease of the MO C=O band intensity. In phorone, for instance, there is one C=O in the condensation product for three acetone molecules, against one for two in mesityl oxide. It would be hazardous to speculate on variations like the ones just mentioned because they accumulate all the experimental errors.

The difference between the sum of the concentration in reaction products and the dose introduced initially is the result of what remains in the gas phase. The decrease of the 58 molecular mass signal with respect to time, shown by the dotted line in Fig. 5A, indicates that, indeed, the reaction is over when the sum of the reagent plus the product reach

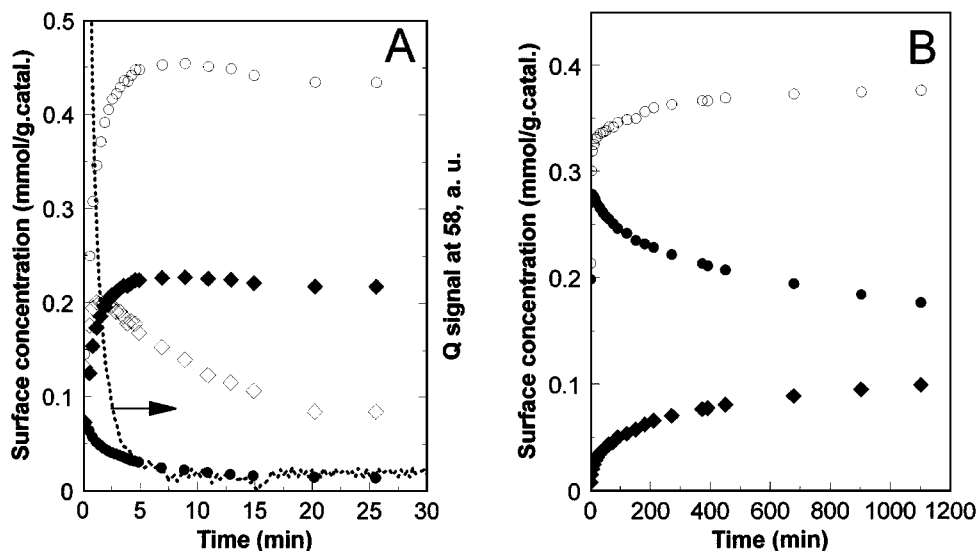


FIG. 5. Balance: $(\text{AcS} + 2^* \text{C}=\text{C})$ surface concentration (\circ), to be compared with the variation with time of the surface concentrations in $\text{C}=\text{C}$ (\blacklozenge) and in CO (\diamond) of MO and in Ac(s) (\bullet). (---) Ac in gas phase. (A) Alumina, (B) USY10F. The total amount of acetone introduced in the IR cell was 0.5 mmol/g catalyst for alumina and 0.4 mmol/g catalyst for USY10F.

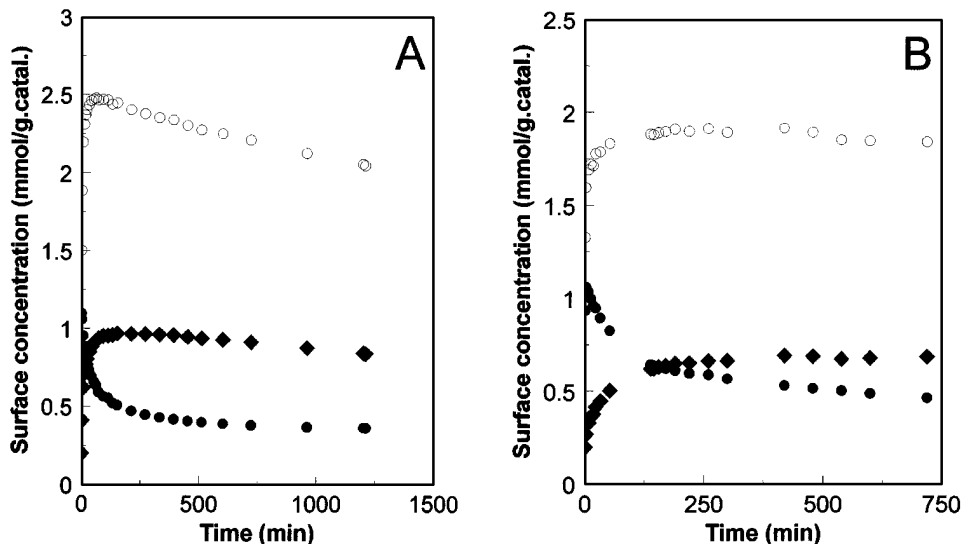


FIG. 6. Balance: $(Ac + 2^*C=C)$ surface concentration (○), to be compared with the variation of the surface concentrations in $C=C$ (◆) of MO and in $Ac(s)$ (●) with time. (A) USY, (B) HM. The total amount of acetone introduced in the IR cell was 3 mmol/g catalyst.

the initial amount of reagent (e.g., ~ 0.4 mmol/g catalyst for the small dose).

For the large doses, there is always an excess of reagent in the gas phase amounting to about 20% of the total transformation. There always remains a fair amount of acetone in the gas phase at the time the yield in MO levels out. The classical explanation for the leveling is that the reaction is poisoned by the reaction product. Here, it would probably be more correct to say that the catalyst is product poisoned. Because mesityl oxide is more basic than acetone, it is more strongly adsorbed by the acid sites, and water in reacting

with coordinately unsaturated aluminum (the Lewis sites) kills the catalyst (28). It has been shown, for instance, that in an alumina similar to that used in this work and calcined at 600°C , the concentration in pentacoordinated alumina decreases from 27 to 9% upon exposure to the atmospheric humidity at room temperature. Similar observations have been made for nonframework aluminum in zeolites (18, 9). On the contrary, water has a negligible effect on the catalytic activity of the Brønsted sites (9).

Figure 7A shows that mesityl oxide on USY is adsorbed at room temperature on Brønsted ($C=C$ stretch at 1560 cm^{-1})

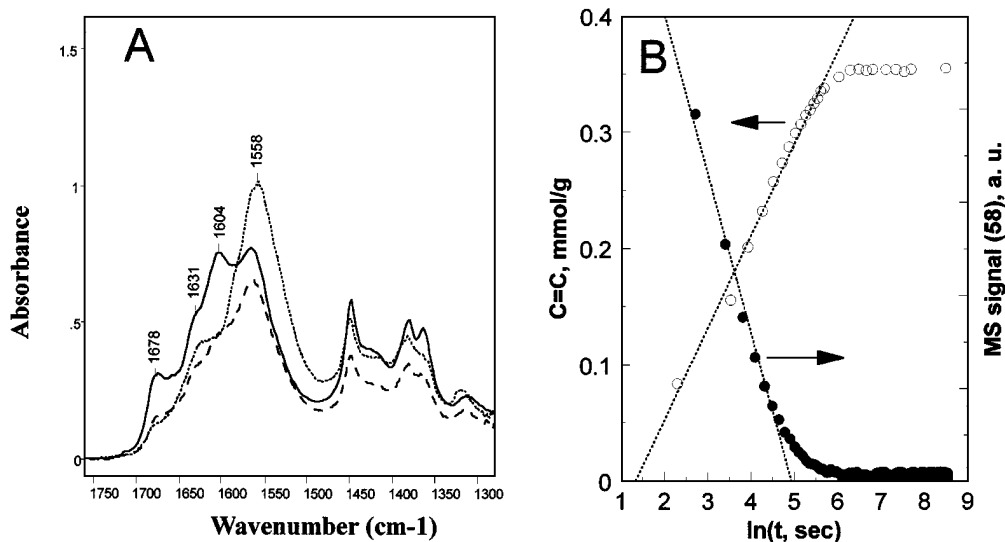


FIG. 7. (A) Adsorption of mesityl oxide at room temperature (—) or at 105°C after a few minutes (---) or after a longer time (---) on USY. (B) Increase of the $C=C$ band intensity at $\sim 1590\text{ cm}^{-1}$ or decrease of the quadrupole signal at mass 58 in the gaseous phase in the presence of alumina (small dose) at 105°C .

TABLE 3

Reaction Rate at Time $t = 1$ min for Ro; Mof (mesityl oxide yield at the end of the reaction); and Acs [amount of adsorbed acetone (all sites) after 1-min reaction]. VAc/VN₂ Is a Measurement of the Availability of the Porous Structure to Acetone: It is the Ratio of Acetone Adsorbed at Saturation, at Room Temperature, to the Volume of N₂ at Saturation at -196°C

Catalyst	Ro ($\mu\text{mol/g/s}$)	Mof (mmol/g)	Acs (mmol/g)	VAc/VN ₂
Alumina ^a	3.59	0.4	0.09	—
USY	1.98	0.97	0.91	0.52
HY(580)	1.12	1.17	0.70	n/a
USY5F	1.05	0.82	0.66	0.41
DHM700 and VG700	0.37	0.34	0.33	0.31
USY10F	0.4	0.39	0.31	0.3
HM	0.33	0.69	1.08	0.67
HY	0.27	0.44	1.72	n/a
HZSM5	0.01	—	—	0.59

^a Small dose; all other experiments were carried out with large doses.

as well as on Lewis (C=C stretch at 1603 cm^{-1}) sites. At 105°C , the intensity of the C=C stretch on the Brønsted sites increases noticeably. The mobility of MO increases at 105°C , and the adsorption on the Brønsted sites is probably more energetic than on the Lewis sites. Consequently, even if MO is formed on Lewis sites, the spectra will show it adsorbed on Brønsted sites. Exactly what type of site is poisoned by the mesityl oxide has to be studied when analyzing the experimental results. As shown in Table 3, the maximum amount of mesityl oxide obtained from the acetone condensation reaction is smaller than the surface concentration in acid sites.

DISCUSSION

On alumina, Fig. 7B shows that the C=C surface concentration and the intensity of the quadrupole mass signal for mass 58 follow opposite linear variation with $\ln t$ and reaches a constant value at $t \simeq 2.5$ min, then the system runs out of reagent. A kinetic law in $\ln t$ suggests that the rate obeys the Elovitch (28) relationship. Here, the rate of adsorption and the rate of transformation are the same and governed by an equation such as

$$\frac{dn}{dt} = a \exp(-\alpha n),$$

where α and a are a function of temperature. A gas phase molecule hitting the surface is transformed into MO after colliding with a molecule activated by a Lewis site.

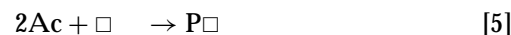
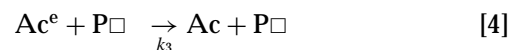
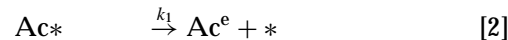
There is too little information to draw conclusions for the reaction kinetics on alumina, except that the reaction rate is much faster than on zeolite and the Lewis sites on the surface of alumina activate acetone energetically.

The situation for zeolite is very different. The rate is conveniently represented as a linear function of the ratio

$$(\text{AcS})(\text{Acw})/\text{MOs}, \quad [1]$$

as shown in Fig. 8. AcS stands for Ac strongly adsorbed by contrast with Acw, which stands for Ac weakly adsorbed. At first sight, the correlations are not impressive, but it must be remembered that the fraction in Eq. [1] is obtained from three independent measurements of AcS, Acw, and MOs.

The carbonyl stretching vibration of AcS is between ~ 1650 and 1690 cm^{-1} , which means (Table 1) that not only acetone on Brønsted site B₁, but also on site B₂ (e.g., the weakly acidic bridging OH groups) is involved. The carbonyl stretching vibration of Acw is between 1690 and 1705 cm^{-1} , thus belonging to acetone adsorbed on Lewis sites and/or the terminal Si-OH. MOs is the surface mesityl oxide adsorbed on Brønsted sites corresponding to the C=C stretch between 1550 and 1565 cm^{-1} . We may account for the linearity of the reaction rate in zeolite with the ratio shown in Eq. [1] in the following way. Let Ac^e be an enol which is the classical reaction intermediate (20). The Lewis (*) and Brønsted (□) sites are covered with acetone or $\text{Ac} + * \rightarrow \text{Ac}^*$ and $\text{Ac} + \square \rightarrow \text{Ac}\square$. Then



Step [2] corresponds to the activation step of acetone into enol by *. Ac□ would be AcS. Thus, Acw could be identified as Ac*. From [3] comes

$$\frac{d(\text{P}\square)}{dt} = k_3(\text{Ac}^e)(\text{Ac}\square).$$

Step [3] is that suggested by Biaglow *et al.* (10). Step [4] corresponds, for zeolites, to the deactivation of enol by the reaction product. From the steady state for Ac^e comes

$$d\text{Ac}^e/dt = 0 = k_1(\text{Ac}^*) - k_2(\text{Ac}^e)(\text{Ac}\square) - k_3(\text{Ac}^e)(\text{P}\square)$$

and finally,

$$\frac{d\text{P}\square}{dt} = k_1 k_2 (\text{Ac}\square)(\text{Ac}^*) / [k_2 (\text{Ac}\square) + k_3 (\text{P}\square)].$$

The latter equation accounts for the observation in Fig. 8A, B if k_2 is smaller than k_3 . Step [3] is the rate-limiting step. Steps [2] and [3] represent the synergy between Lewis and Brønsted sites. Thus, the activation would

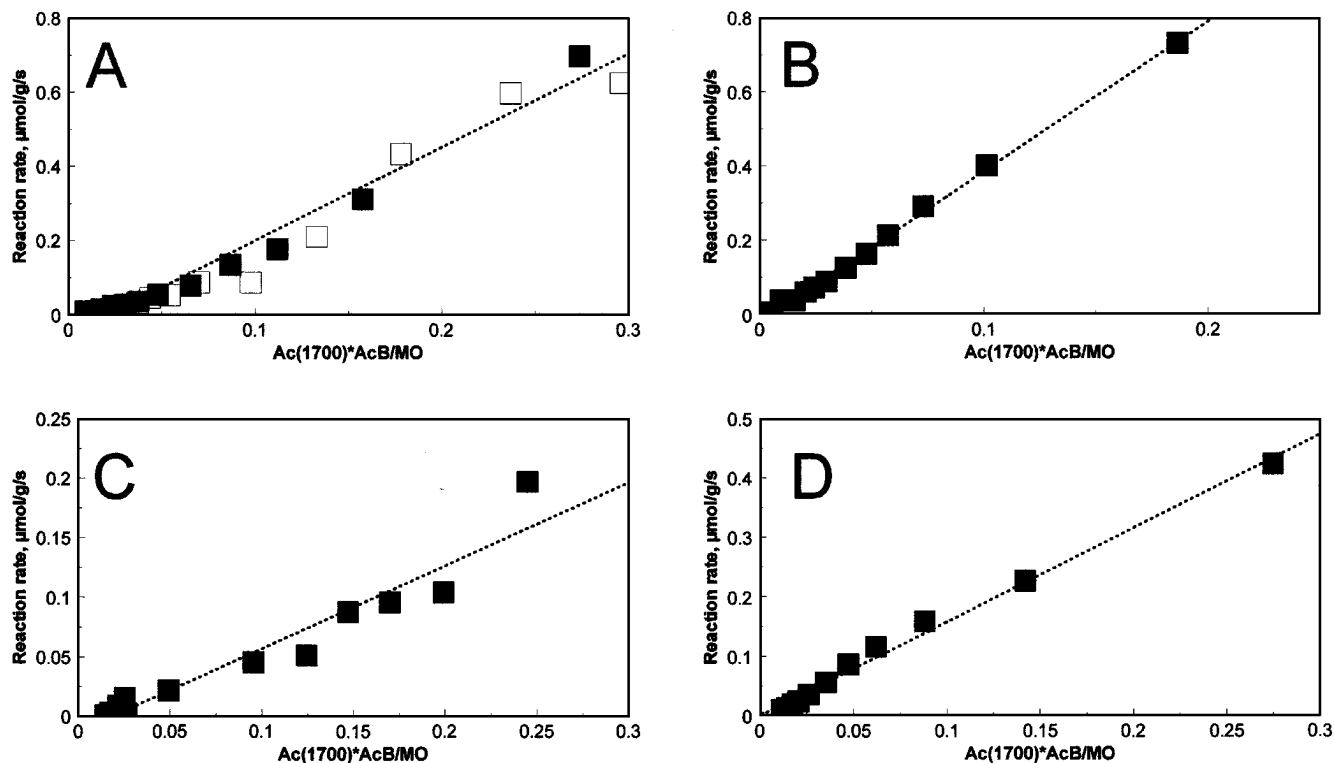


FIG. 8. Reaction rate expressed in function of the ratio Ac(w) Ac(S)/MO on USY (A), USY5F (B), HM (C), and USY10 (D). Large dose at 105°C. Two different sets of results are shown for USY in (A).

occur on Lewis sites. In zeolites, these sites would be on nonframework alumina.

This hypothesis has multiple consequences. First, there should be a relationship between the rate of the reaction and the surface density in Lewis sites. This is suggested by Fig. 9A, whereas the absence of correlation with the sur-

face density in Brønsted sites is shown in Fig. 9B. Also, the reaction is "stoichiometric" in the sense that water kills the catalytic sites. By comparing data in Tables 2 and 3, it can be seen that the maximum yield in MO, that is MO_f, is always lower than the initial number of Lewis sites (except in USY5F where it is slightly higher). The synergy

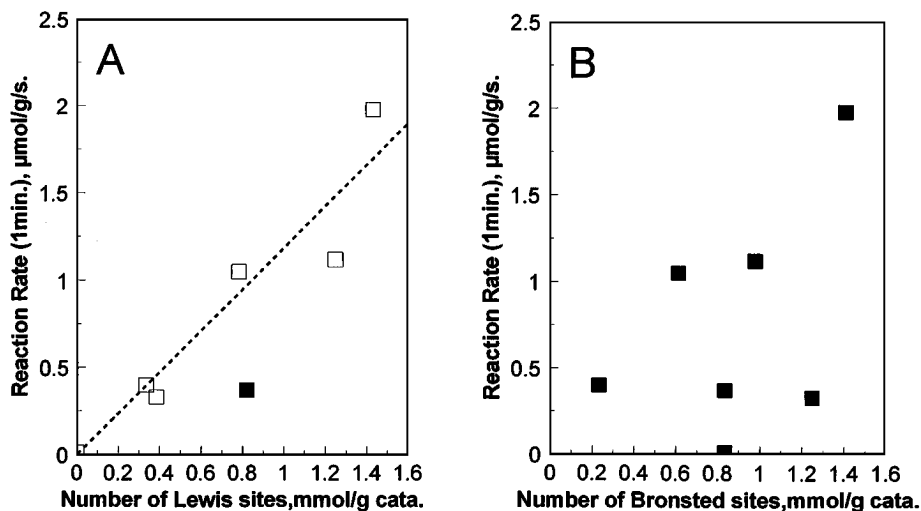


FIG. 9. Reaction rate R_0 (after 1 min reaction) on zeolites expressed vs. the number of Lewis sites (A) or Brønsted sites (B). The black square in (A) is the reaction rate observed for two experiments on H-mordenite, dealuminated at 700°C.

implies that both types of acid sites are spatially close to one another.

Finally, a major difference between alumina and zeolite comes from the fact that in alumina, the gas phase acetone is probably involved, whereas on zeolite, condensation occurs between acetone adsorbed on two different kinds of sites. The influence of the gas phase is indirect because of the equilibrium between Acw and the gas phase.

CONCLUSIONS

The condensation of acetone on mesityl oxide is a bimolecular reaction between acetone activated on a Lewis site and acetone adsorbed on bridging OH zeolites. The turnover per Lewis sites is on the order of 10^{-3} reactions per site and per second at 105°C , and it is constant for all zeolites. On alumina, it seems that the reaction occurs between a molecule in the gas phase and a molecule activated on a Lewis site. In addition, the condensation goes further than mesityl oxide.

On zeolites and at 105°C , the extent of the further condensation reaction is much smaller. On both zeolites with nonframework aluminum and alumina, the catalyst gets "product poisoned" by MO and, also, perhaps, by water.

ACKNOWLEDGMENTS

This work has been made possible by DOE grant DOE-FG02-90 ER1430. We want to thank the referees for interesting comments.

REFERENCES

1. Lercher, J. A., *Z. Phys. Chem. N. F.* **129**, 209 (1982).
2. Hanson, B. E., Wieserman, L. F., Wagner, G. W., and Kaufman, R. A., *Langmuir* **3**, 549 (1987).
3. Anderson, J. A., and Rochester, C. H., *J. Chem. Soc., Faraday Trans. 1* **85**, 1129 (1989).
4. McManus, J. C., Harano, Y., and Low, M. J. D., *Can. J. Chem.* **47**, 2545 (1969).
5. Dao, T. V., Kitaev, L. E., Topchieva, K. V., Kubasov, A. A., and Ratov, A. N., *Vestnik Mosk. Universiteta, Khimiya* **26**, 65 (1971).
6. Kubelková, L., Čejka, J., and Nováková, J., *Zeolites* **11**, 48 (1991).
7. Kubelková, L., and Nováková, J., *Zeolites* **11**, 822 (1991).
8. Bell, V. A., and Gold, H. S., *J. Catal.* **79**, 286 (1983).
9. Xu, T., Munson, E. J., and Haw, J., *J. Am. Chem. Soc.* **116**, 1962 (1994).
10. Biaglow, A. I., Šepa, J., Gorte, R. J., and White, D., *J. Catal.* **151**, 373 (1995).
11. Biaglow, A. I., Gorte, R. J., Kokotailo, G. T., and White, D., *J. Catal.* **148**, 779 (1994).
12. Šepa, J., Lee, C., Gorte, R. J., Kassab, E., Evleth, E. M., Jessri, M., Allavena, M., and White, D., *J. Phys. Chem.* **100**, 18515 (1996).
13. Kubelkova, L., Kotria, J., Florian, J., Bolom, T., Fraissard, J., Heribout, L., and Doremieux-Morin, C., *11th Intern. Congress on Catalysis* **101**, 761 (1996).
14. Panov, A. G., and Fripiat, J. J., *Langmuir*. [submitted]
15. Hair, M. L., "Infrared Spectroscopy in Surface Chemistry," p. 149. Dekker, New York, 1967.
16. Hong, Y., Gruver, V., and Fripiat, J. J., *J. Catal.* **161**, 766 (1996).
17. Gruver, V., Panov, A., and Fripiat, J. J., *Langmuir* **12**, 2505 (1996).
18. Blumenfeld, A. L., Coster, D., and Fripiat, J. J., *J. Phys. Chem.* **99**, 1581 (1995).
19. Blumenfeld, A. L., and Fripiat, J. J., *Topics in Catalysis* **4**, 119 (1997).
20. Farcasiu, D., Ghenciu, A., and Miller, G., *J. Catal.* **134**, 118 (1992).
21. Hong, Y., and Fripiat, J. J., *Microporous Materials* **4**, 323 (1995).
22. Hong, Y., Gruver, V., and Fripiat, J. J., *J. Catal.* **150**, 421 (1994).
23. Coster, D., and Fripiat, J. J., *Chem. Materials* **5**, 1204 (1993).
24. Yin, F., Blumenfeld, A. L., Gruver, V., and Fripiat, J. J., *J. Phys. Chem. B* **101**, 1824 (1997).
25. Coster, D., Blumenfeld, A. L., Gruver, V., and Fripiat, J. J., *J. Phys. Chem.* **98**, 6201 (1994).
26. Gruver, V., and Fripiat, J. J., *J. Phys. Chem.* **98**, 8549 (1994).
27. Panov, A. G., Gruver, V., and Fripiat, J. J., *J. Catal.* **168**, 321 (1997).
28. Coster, D. J., Fripiat, J. J., Muscas, M., and Auroux, A., *Langmuir* **11**, 2615 (1995).
29. Roginski, S. S., in "Adsorption und Katalyse in homogen Oberflächen." Akademie Verlag, Berlin, 1958.